Supplementary information

Bioinspired Anion Exchange Membrane with Steric Cross-linking Centers for Industrial-scale Water Electrolysis

Tang Tang[1,2 †], Husileng Lee[1,2 †], Zhiwei Wang[1,2 †], Zhiheng Li[1,2], Linqin Wang[1,2], Dexin Chen[1,2], Wentao Zheng[1,2], Qinglu Liu[1,2], Lanlan He[1,2], Guoheng Ding[1,2], Ziyu Tian[1,2], Licheng Sun[1,2,3*]

[1]*Center of Artificial Photosynthesis for Solar Fuels and Department of Chemistry, School of Science and Research Center for Industries of the Future, Westlake University, Hangzhou 310024, China.*

[2]*Institute of Natural Sciences, Westlake Institute for Advanced Study, Hangzhou 310024, China.*

[3] *Division of Solar Energy Conversion and Catalysis at Westlake University, Zhejiang Baima Lake Laboratory, Hangzhou 310000, Zhejiang Province, China.*

*Correspondence to:

Licheng Sun: sunlicheng@westlake.edu.cn

†These authors contributed equally to this work.

Experimental Procedures

Materials

P-terphenyl (98%), triptycene (98%), 9,9'-spirobifluorene (98%), 1-Methyl-4-piperidone (99%), and methyl iodide (CH_3I, 99%) were supplied by Adamas. Trifluoroacetic acid (TFA) (98%), and trifluoromethanesulfonic acid (TFSA) (98%) were supplied by Innochem. Ethyl ether, ethyl acetate (EA), and ethanol were supplied by Titan. Potassium hydroxide (KOH), and potassium carbonate (K_2CO_3) in the analytical grade were purchased from Leyan. DMSO-d_6 (99.9%) and D_2O (99.9%) were purchased from Cambridge Isotope Laboratories. Among them, the dichloromethane was treated with anhydrous sodium sulfate before use while the other reagents were used directly.

Characterizations

^1H nuclear magnetic resonance (^1H NMR) spectra were recorded on Bruker 510 instrument in a standard solvent of DMSO-d_6 to confirm the chemical structure. The carbon dioxide (CO_2) sorption was performed on Micromeritics 3-Flex at 273.15 K. The Nitrogen (N_2) sorption was performed on Micromeritics 3-Flex at 195.15 K. Atomic force microscopy (AFM) detected the surface morphology on Dimension ICON (Bruker) with tapping mode. Scanning electron microscope (SEM) image of the cross-sectional morphology was detected using Gemini500 (Zeiss). The molecular weight of polymers was recorded on Advanced Polymer Chromatography (Waters) using DMF as the solvent. Positron annihilation lifetime spectroscopy (PALS) (Thermo Fisher Scientific, America) was used to obtain the microcavity size and free volume in the AEMs.

Synthesis of the polymers

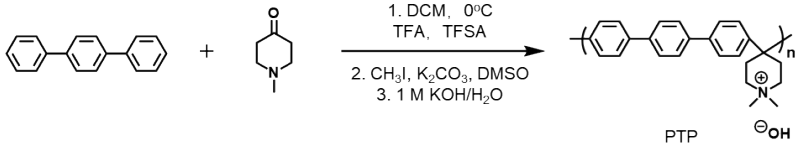

Scheme S1. Synthesis route of PTP.

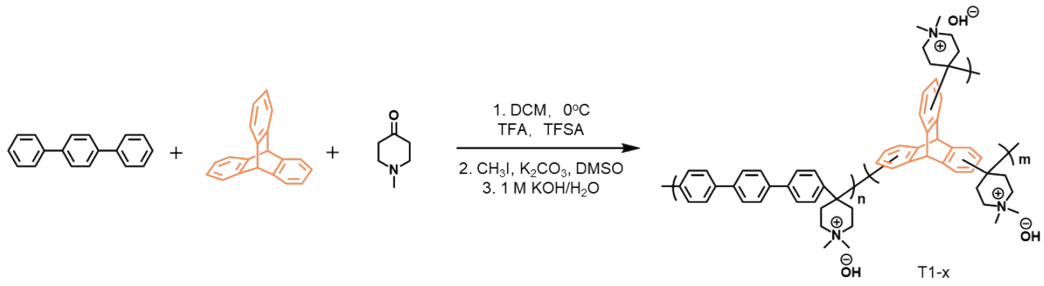

Scheme S2. Synthesis route of T1-x. Note: the x of T1-x refers to the theoretical molar percentage of Trp /(Trp+p-terphenyl) in the polymer.

Scheme S3. Synthesis route of T2-x. Note: the x of T2-x refers to the theoretical molar percentage of Sp /(Sp+biphenyl) in the polymer.

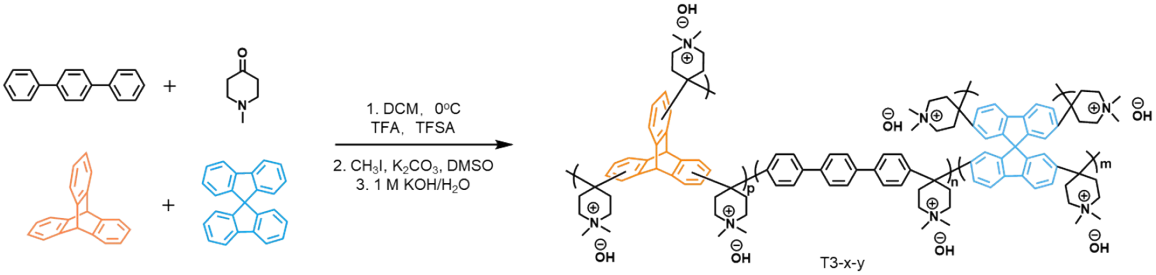

Scheme S4. Synthesis route of T3-x-y. Note: the x and y of T3-x-y refers to the theoretical molar percentage of Trp /(Trp+p-terphenyl) and Sp/(Sp+p-terphenyl) in the polymer.

Poly(p-terphenyl triphenylmethane 1-methyl piperidine) (PTP) was prepared by an electrophilic substitution reaction (**Scheme S1**). P-terphenyl (2.0 g), and N-methyl-4-piperidone (1.2 mL) were dissolved in dichloromethane (10.0 mL) under stirring. The temperature was lowered to 0 °C before TFA (1.0 mL) and TFSA (10.0 mL) were slowly added. Nine hours later, the mixture became so viscous that the magnetic stirrer bar could not rotate. The viscous mixture was precipitated in a solvent mixture of 2 M K_2CO_3 with a methanol to H_2O ratio of 1:1 (v/v). Then, the precipitate was chopped and purified three times consecutively with deionized water (DIW) and EA. After that, the white product was dried in an oven at 80 °C.

T1-1.0 was synthesized via the showed procedure (**Scheme S2**). P-terphenyl (2.0 g), triptycene (22.0 mg), and N-methyl-4-piperidone (1.20 mL) were dissolved in dichloromethane (10.0 mL) under stirring. The temperature was lowered to 0 °C before TFA (1.0 mL) and TFSA (10.0 mL) were slowly added. The mixture became so viscous that the magnetic stirrer bar could not rotate. The viscous mixture was precipitated in a solvent mixture of 2 M K_2CO_3 with a methanol to H_2O ratio of 1/1 (v/v). Then the precipitate was chopped and purified three times with DIW and EA consecutively. After that, the white product was dried in an oven at 80 °C for 48 hours. T2-1.0 was synthesized by a similar procedure except for the use of 9,9'-spirobifluorene instead of triptycene (**Scheme S3**).

T3-1.0-0.5 was synthesized as follows (**Scheme S4**): P-terphenyl (2.0 g), triptycene (22.0 mg), 9,9'-spirobifluorene (13.7 mg) and N-methyl-4-piperidone (1.20 mL) were dissolved in dichloromethane (10.0 mL) under stirring. The temperature was lowered to 0 °C before TFA (1.0 mL) and TFSA (10.0 mL) were slowly added. The mixture became so viscous that the magnetic stirrer bar could not rotate. The viscous mixture was precipitated in a solvent mixture of 2 M K_2CO_3 with a methanol to H_2O ratio of 1/1 (v/v). Then the precipitate was chopped and purified three times with DIW and EA consecutively. After that, the white product was dried in an oven at 80 °C for 48 hours.

Synthesis of cationic polymers

A typical quaternization method for polymers in I^- state polyelectrolyte involved the following steps: first, the precursor (1.0 g) was dissolved in 10 mL of DMSO. Then, 0.47 g of K_2CO_3 was added to the solution. To ensure complete quaternization, an excess of CH_3I (1.0 mL) was added. The reaction mixture was allowed to react for 24 hours at 25 °C. After the reaction, a precipitate formed when the reaction solution was dropped into a mixture of ethyl ether and methanol ($v_{ethyl\ ether}$ /$v_{methanol}$ = 6:1). To purify the product, it was subjected to three rounds of purification. Each round involved washing the product with EA and DIW in succession. Finally, the product was filtered to obtain a yellow solid.

Membrane preparation

Under stirring, 100 mg of polyelectrolytes and 5 mL of DMSO were added to a glass bottle. Once the polymers had completely dissolved, the solution was filtered and poured onto a glass plate. The resulting membrane was then dried in a vacuum oven at 90 °C for 1 hour, followed by 100 °C for 1 hour, and finally at 120 °C for 3 hours. To obtain the hydroxide form of the T1-1.0 membrane, 1.0 g of the membrane was subjected to ion exchange in a 1M KOH solution at 80 °C for more than five cycles, with each cycle lasting 2 hours. Afterward, the membrane was washed and immersed in deaerated deionized water under N_2 to prevent contact with CO_2 and the formation of carbonate.

Ion exchange capacity (IEC) testing

The IEC of membranes was tested through Mohr's titration. Typically, the dried AEMs in hydroxide form were soaked in 0.01 M HCl solution for 48 hours to complete the anion exchange. Subsequently, 0.01 M NaOH was added to the remaining HCl solution until reaching a phenolphthalein endpoint. This operation was repeated three times for accuracy. The IEC can be calculated using equation (1):

$$IEC = \frac{C_1V_1 - C_2V_2}{M_{dry}} \quad (1)$$

where the original concentrations and volumes of HCl solution and NaOH solution are C_1 (M) and V_1 (mL), C_2 (M) and V_2 (mL), respectively. M_{dry} represents the weight of the AEMs after drying.

Water uptake (WU) and swelling ratio (SR)

Membranes in hydroxide form with a size of 2 cm × 2 cm were immersed in DIW at 25 °C, 40 °C, 60 °C, and 80 °C separately. After being taken out, the surface water was quickly wiped off, and the mass and length were recorded as W_{wet} and L_{wet}, respectively. Then, the membranes were dried in an oven at 80 °C for one day, and the mass and length were recorded as W_{dry} and L_{dry}, respectively. Equations (2) and (3) can be used to obtain the WU and SR.

$$WU = \frac{W_{wet} - W_{dry}}{W_{dry}} \times 100\% \qquad (2)$$

$$SR = \frac{L_{wet} - L_{dry}}{L_{dry}} \times 100\% \qquad (3)$$

The hydration number (λ) can be obtained from eq (4):

$$\lambda = \frac{WU(\%) \times 10}{IEC \times 18} \qquad (4)$$

Ionic conductivity

This device is a modified version of a spiral micrometer, featuring two platinum plate electrodes attached to each end. The measurement procedure is as follows: Firstly, the AEM was immersed in a 1 M KOH solution for 6 hours at 80 °C, followed by an additional 2 hours at room temperature. The KOH solution was replaced every 2 hours. This immersion process led to the replacement of the initial counterion in the AEM with OH^- ions. After the immersion, the AEM was washed with N_2-saturated water in a glovebox while continuously being blown with N_2. Subsequently, the AEM was installed on a homemade device and soaked in N_2-saturated water (Figure S5). The

temperature was gradually increased from room temperature to 80 °C, and the test frequency range applied was from 1×10^{5} Hz to 1×10^{-1} Hz. The ohmic resistance and thickness of the AEM were directly measured at temperatures of 25 °C, 40 °C, 60 °C, and 80 °C. Then, using equation 1, the OH− conductivity was calculated according to eq 1.

$$\sigma = \frac{d}{RS} \tag{5}$$

In eq(5), σ is the through-plane OH^- conductivity of AEM, d is the effective distance between platinum electrodes, which equals the thickness of AEM. It was directly read from the spiral micrometer. R is the ohmic resistance of the AEM, S is the area of the platinum electrode.

Thermal stability and mechanical property

The thermal stability of the membranes was measured by a thermogravimetric Analyzer (Mettler-Toledo) under an N_2 atmosphere. Samples were heated from 30 to 500 °C with a heating rate of 10 °C min^{-1}.

The mechanical property of 2 mm × 15 mm strips of membranes was evaluated using a dynamic thermomechanical analyzer (Discovery DMA 850, LHB21051806, TA-Waters, USA) with a preload force of 0.01 N and ramp rate of 0.5 mm min^{-1}.

Morphology

The microphase morphologies of membranes (OH^- form) were observed using atomic force microscopy (AFM, Dimension ICON, Bruker, USA) in tapping mode at room temperature.

Alkali stability

The samples were soaked in 1 M KOH at 80 °C for 1500 h or in 5 M KOH at 80 °C for 500 h, and the ionic conductivity of the membranes was constantly tested to monitor their alkali stability. In addition, the reasons for the decrease of OH^- conductivity of membranes were investigated by ^1H NMR spectra.

Nanoindentation and Nanoscratch Testing

The Nanoindentation and Nanoscratch Testing was measured by Hysitron TI 980 TriboIndenter. Nanomechanical Indentation Testing: The specimen is placed on a nanomechanical indentation instrument for indentation testing. The maximum load is set at 10 mN and the loading rate is 1 mN s^{-1}. The maximum load is maintained for 5 seconds during the loading process, followed by unloading at the same rate. Nanomechanical Scratching Testing: A certain normal force is applied to the indenter, which is then moved along the surface of the sample. The test measures the friction force and coefficient of friction of the sample surface.

Preparation of Pt/C cathodic catalysts

20 mg of 60 wt.% Pt/C powder was dispersed in a 4.0 mL mixture of isopropyl alcohol and ultrapure water in a 1:1 ratio. Then, 80 μL of 5 wt.% Nafion solution was added and the mixture was sonicated for 1 hour to form a homogeneous ink. A definite volume of the ink (with a loading mass of 1.0 mg cm^{-2}) was sprayed onto the surface of a 16 cm^2 carbon fiber paper (CP) to form a gas diffusion electrode and dried at room temperature.

Synthesis of Ni-Mo cathodic catalysts

The catalyst was synthesized based on previously reported literature.[S1] Briefly, a piece of cleaned NF (3 cm × 2 cm) was put into 25 mL solution containing $Ni(NO_3)_2{\cdot}6H_2O$ (40 mM) and $(NH_4)_6Mo_7O_{24}{\cdot}4H_2O$ (10 mM) in the Teflon autoclave. Then, the autoclave was heated at 150 °C for 6 h in an oven. After the reaction, the electrode was washed with DI water, and ethanol, and dried at 50 °C. Finally, the precursor was heated at 500 °C for 2 h in H_2/Ar (5:95) atmosphere.

Synthesis of Ni-Fe@NF anodic catalysts

The catalyst was synthesized based on previously reported literature with modification.[S2] Briefly, a piece of cleaned NF (3 cm × 2 cm) was hung by stainless steel wire and immersed into a sample vial (25 mL) containing aqueous solution of

$Ni(NO_3)_2·6H_2O$ (30 mM) and $Fe(NO_3)_3·9H_2O$ (10 mM). The growth of catalysts was conducted at room temperature for 72 h. After that, the electrode was washed with DIW and ethanol, and dried in a vacuum.

Water electrolysis performance testing

The MEA was assembled with Ni-Fe@NF catalyst, T1-1.0, and Pt/C@CP or Ni-Mo@NF catalyst. The performance of T1-based AEM-WE was studied with 1 M KOH as electrolyte. The J-V curve at different temperatures (from 25 °C to 80 °C) over an applied voltage range of 1.0–2.0 V was recorded. The linear sweep voltammetry measurements were performed at a scan rate of 5 mV s^{-1}. The electrolyte resistance (R) was monitored at 1.6 V in the frequency from 100 kHz to 0.1 Hz at different temperatures. The single-cell durability was conducted at a constant current density of 1.0 A cm^{-2} with 1 M KOH feed at different temperatures.

The AEM-WE was measured using the Autolab PGSTAT302 workstation (with a 20 A booster) with a KOH flow rate of 60 mL min^{-1}. The temperature of the KOH solution was controlled by two temperature sensors located in the bipolar plates, which were positioned very close to the flow field.

The general methodology for polymer simulation

A multiscale computational approach was employed to investigate the pore architecture of membranes and the transfer behavior of water and hydroxide within the nanochannels. Initially, amorphous polymer models, including PTP and T1-1.0, were constructed to analyze the distribution of pore sizes (PSD). Subsequently, classical molecular dynamics (MD) simulations were utilized to investigate the diffusion coefficient of water and hydroxide ions within the membrane. The following section provides a detailed description of the computational methods.

Model Construction

All computational models were manually constructed using the free visualization software Discovery Studio Visualizer [S3]. There are a total of two computational

models. In the T1 polymer system, 20 polymer chains were involved, with each chain containing only one triptycene molecule. The triptycene molecule is connected to three identical side chains, each consisting of 33 *p*-terphenyl molecules. Near each *p*-terphenyl monomer, 1 hydroxide ion and 7 water molecules are placed based on experimental data. The total number of atoms in the system is 149,180. In the PTP system, there is no triptycene and only 20 polymer chains with a polymerization degree of 60 are present. Near each p-terphenyl monomer, 1 hydroxide ion and 5 water molecules are placed. The total number of atoms in the system is 82,840. The localized structural diagram of the initial model is as follows:

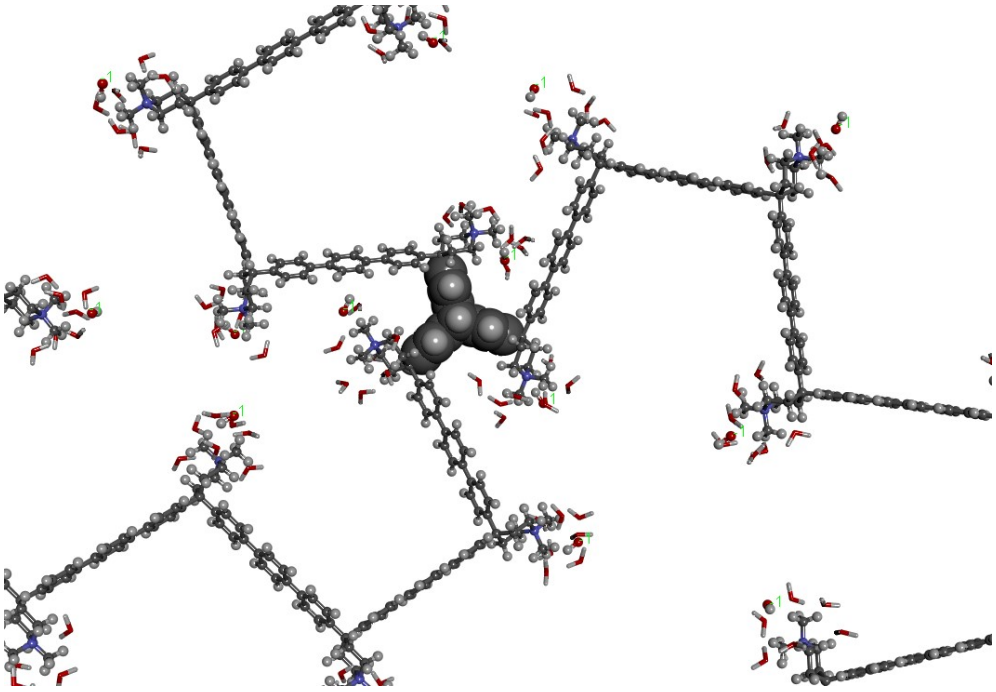

Molecular dynamics simulation setup

All molecular dynamics (MD) simulations were performed using the NAMD 2.14 software package[S4]. The molecular force field for the polymer monomers was obtained from the CGenFF force field[S5]. The TIP3P water model was applied to describe water molecules in the system. The cutoff distance for short-range non-bonded interactions was gradually decreased to 0 in the distance range from 10 to 12 angstroms. The pair list search radius was set to 14 angstroms. Periodic boundary conditions were applied

during the MD simulation. Long-range electrostatic interactions were calculated using the PME method[S6]. The temperature in the MD simulation was set to 298K with the Langevin thermostat[S7]. Before the dynamic simulation, a 50000-step energy minimization of conjugate gradient (CG) was performed to eliminate high-energy contacts in the system. Subsequently, an initial equilibration simulation of 5 ns was carried out with a time step of 1 fs to obtain a relatively stable simulation system. Following that, the integration time step was switched to 2 fs and the SHAKE algorithm[S8] was used to constrain all bonds involving hydrogen atoms. The Langevin piston method[S9] was employed for pressure control to adjust the system volume and stabilize the density within the range consistent with experimental values. After the system was stable, a total of 400 ns production simulation was performed under an isothermal-isobaric (NPT) ensemble, with a temperature of 298K and a pressure of 1 bar. The resulting MD trajectories from the production phase were used for the subsequent analysis.

Computational methods for triptycene center-based unit and 9,9'-spirobifluorene center-based unit optimizations

The optimizations were performed for the two molecules under the level of hybrid density functional theory (DFT) B3LYP with the basis set 6-31G(d, p) via Gaussian 16. C. 01 version. The D3 version of Grimme's dispersion was considered. Then, the vibrational frequencies of the molecule were calculated and no imaginary frequency was found.

Computational methods for triptycene center-based unit and 9,9'-spirobifluorene center-based unit optimizations

The optimizations of the systems (T1-1.0, T2-1.0, and T3-1.0-1.0) were performed via GFN force field, respectively. The study systems include copolymer, OH^- and water molecular (added based on water adsorption). The T1-1.0 system consists of 99 *p*-terphenyl molecules and one Trp unit. The T2-1.0 system consists of 99 *p*-terphenyl molecules and one Sp unit. The T3-1.0-1.0 system consists of 98 *p*-terphenyl molecules,

one Trp unit, and one Sp unit.

Analysis

All trajectory visualizations were performed using VMD [S10]. The physical quantity PSD (Pore Size Distribution), which characterizes the features of hydrophilic channels, was analyzed and calculated using the Poreblazer (v4.0) software [S11].

The diffusion coefficient for water molecules and hydroxide ions were calculated using the Diffusion Coefficient Tool plugin in VMD [S12]. The diffusion of small species, such as water and ions in polyelectrolyte membranes, is a complex atomistic-level phenomenon with multiple facets. To assess the mobility of water and anions, we calculated the self-diffusion coefficient by analyzing the linear part of the mean-squared displacement (MSD) plot, employing Einstein's relation for n-dimensional Brownian motion (eq (6)).

$$M(\tau) = \langle |r(\tau) - r(0)|^2 \rangle \qquad \text{eq (6)}$$

Where $r(\tau)$ indicates the position of a particle at time τ, and the angle brackets indicate an average over all particles of the species under analysis. In practice, to improve convergence, the MSD analysis is repeated using different time origins, under the equilibrium assumption. If the system is in a diffusive regime and the position measurement error is negligible, the diffusion coefficient can be obtained through Einstein's relation:

$$D_a(\tau) = \mathrm{M}(\tau)/2\mathrm{E}\tau \qquad \text{eq (7)}$$

Where E is the dimensionality of the system (integer, $1 < E < 3$). In general, MSD values at multiple lag times are computed from the same trajectory to check their linearity and asymptotic slope in τ to check diffusivity and average out measurement errors.

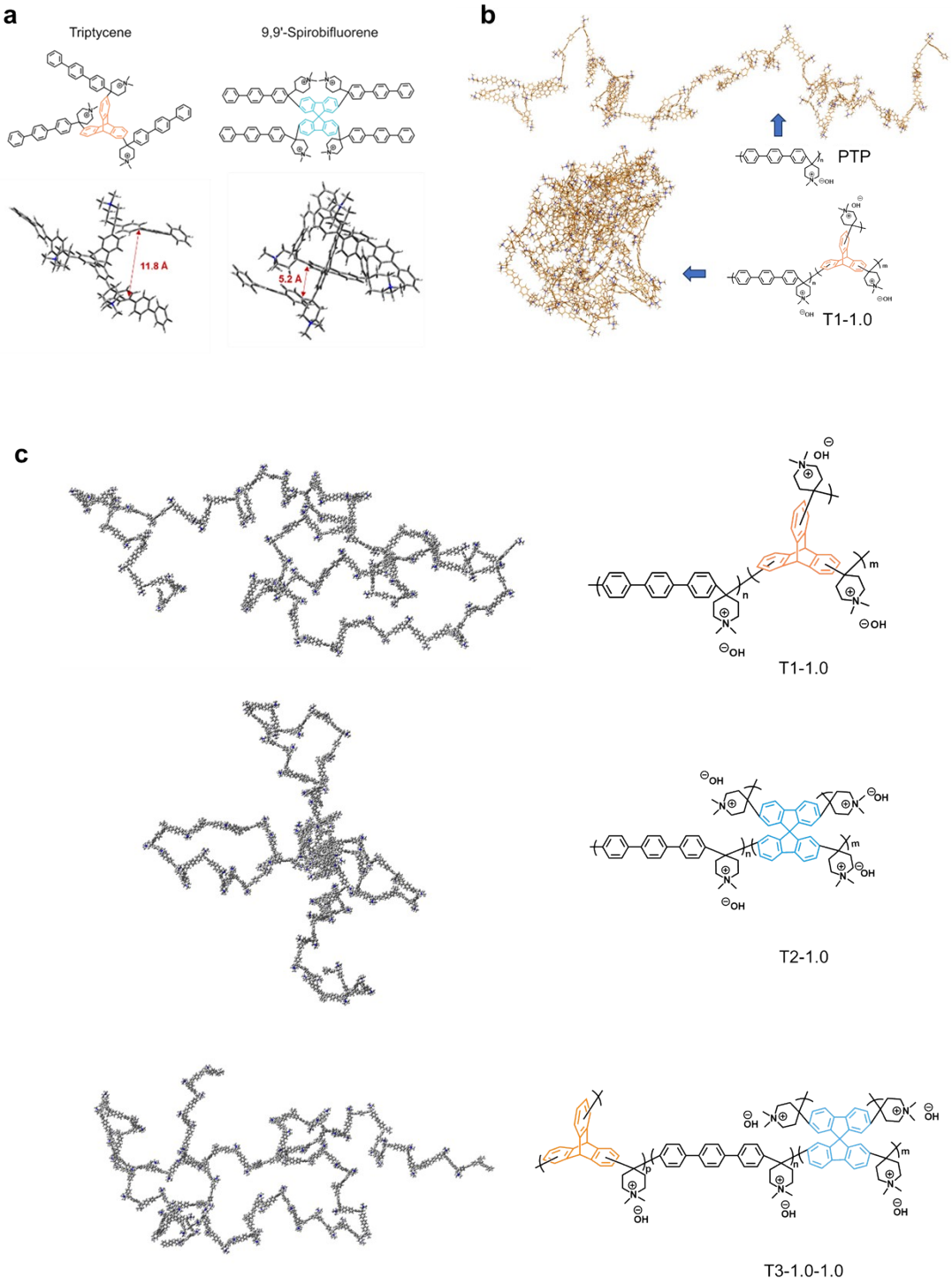

Figure S1. (a) The 3D view of the spatial models of triptycene center-based unit (left), 9,9'-spirobifluorene center-based unit (right). (b) The 3D view of the extracted single molecular chains in the simulated units PTP (**Figure 3a. PTP**) and T1-1.0 (**Figure 3a. T1-1.0**). (c) The 3D view of the spatial structures of T1-1.0, T2-1.0 and T3-1.0-1.0.

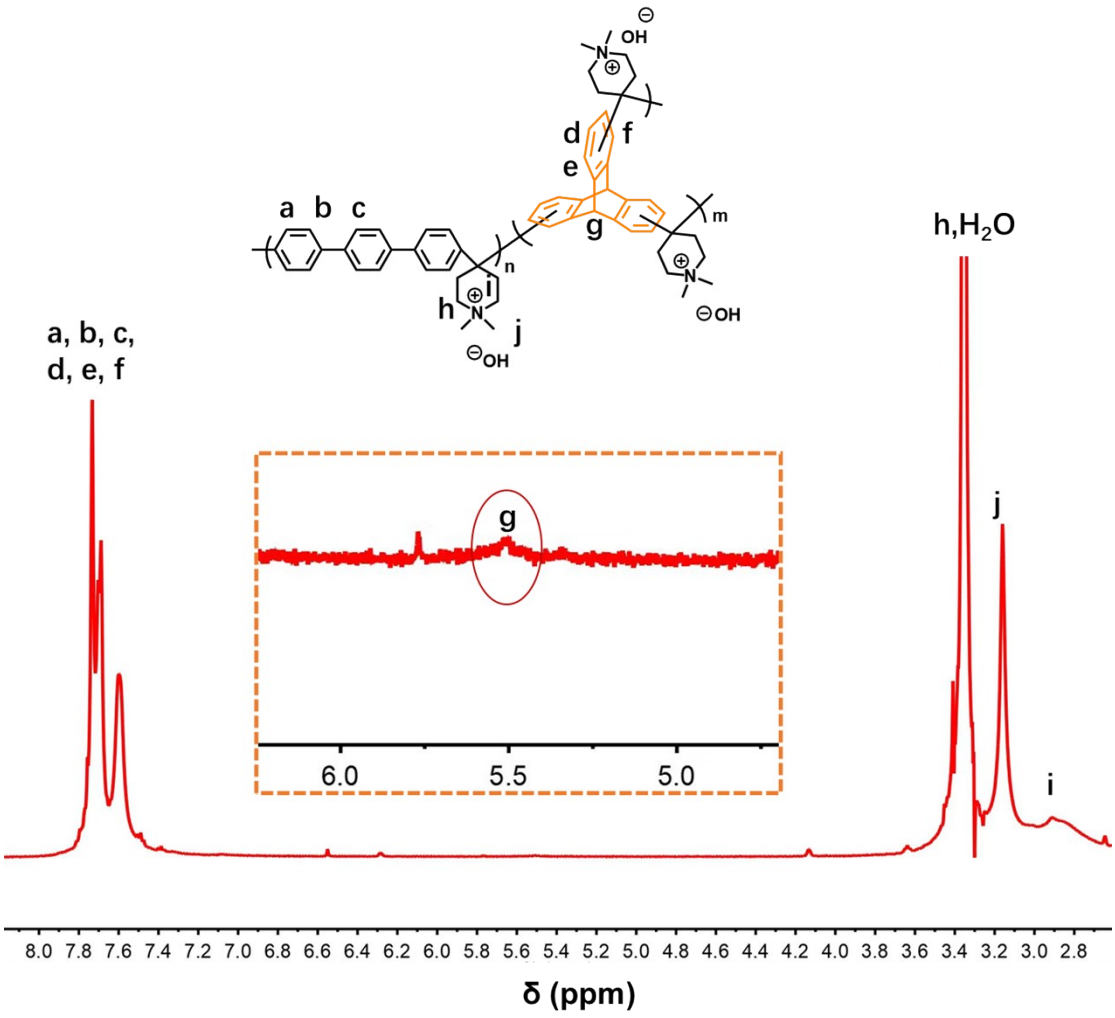

Figure S2. ^{1}H NMR spectrum of T1-1.0, DMSO-d_6 as the solvent (feed ratio: Trp is present at a feed ratio of 1 mol% relative to aromatic hydrocarbon monomers in the polymerization).

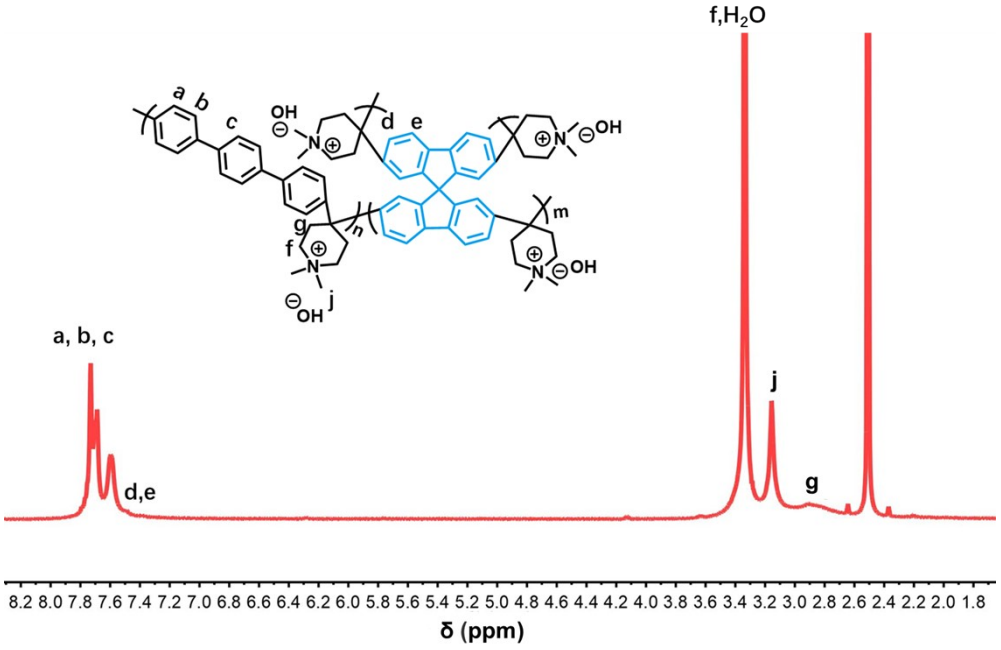

Figure S3. ^{1}H NMR spectrum of T2-1.0, DMSO-d_6 as the solvent (feed ratio: Sp is present at a feed ratio of 1 mol% relative to aromatic hydrocarbon monomers in the polymerization).

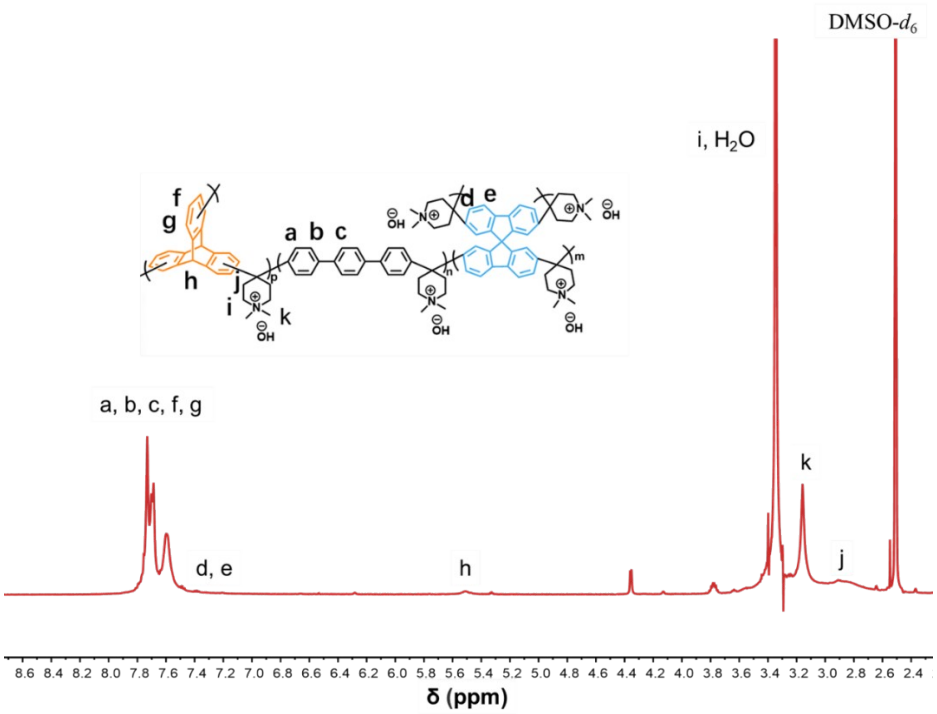

Figure S4. ^{1}H NMR spectrum of T3-1.0-1.0, DMSO-d_6 as the solvent (feed ratio: Sp is present at a feed ratio of 1 mol% relative to aromatic hydrocarbon monomers in the polymerization; Trp is present at a feed ratio of 1 mol% relative to aromatic hydrocarbon monomers in the polymerization).

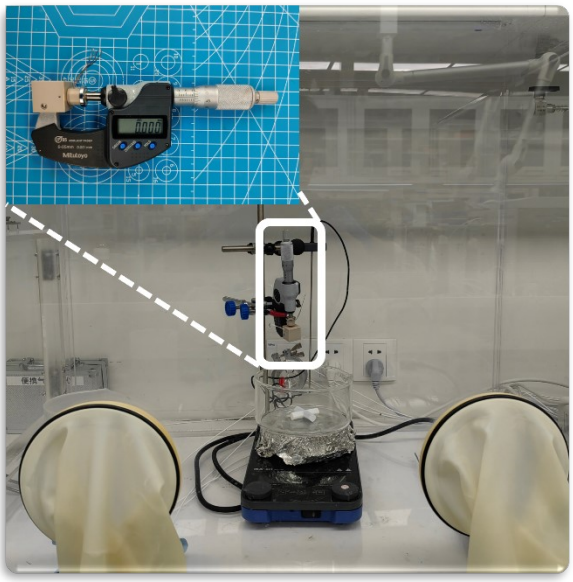

Figure S5. Home-made set-up for ion conductivity testing.

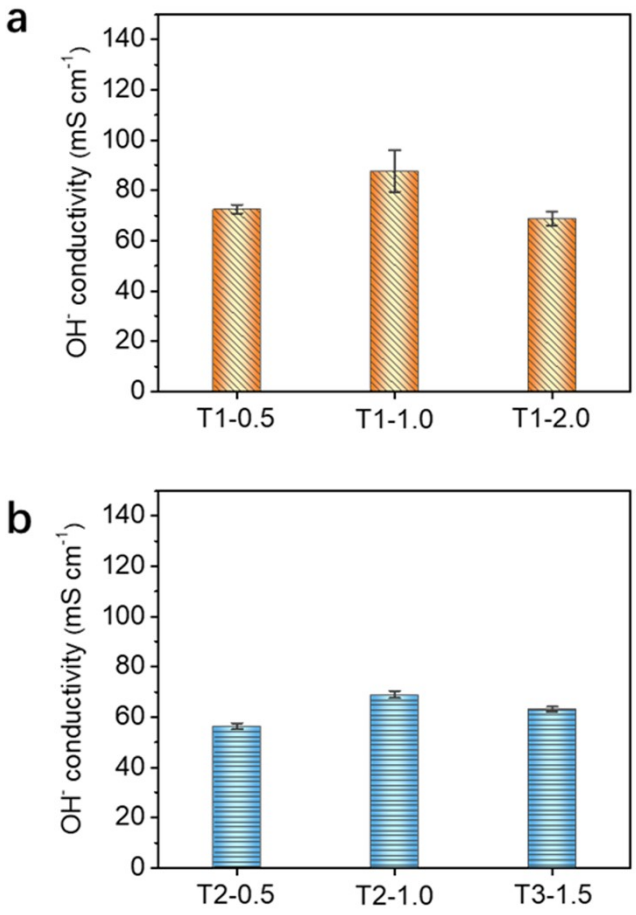

Figure S6. (a)The through-plane ion conductivities of afforded T1-AEMs with different Trp ratios at room temperature. (b) The through-plane ion conductivities of afforded T2-AEMs with different Sp ratios at room temperature.

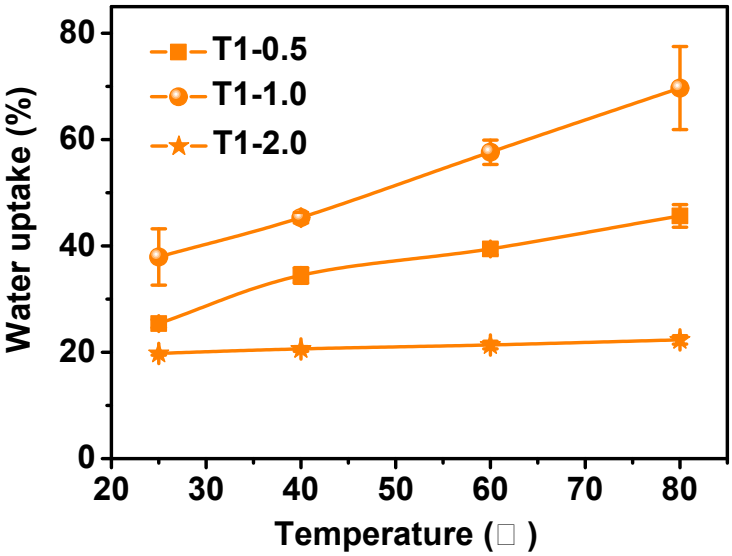

Figure S7. The water uptake of afforded T1 AEMs with different Trp ratios at different temperatures.

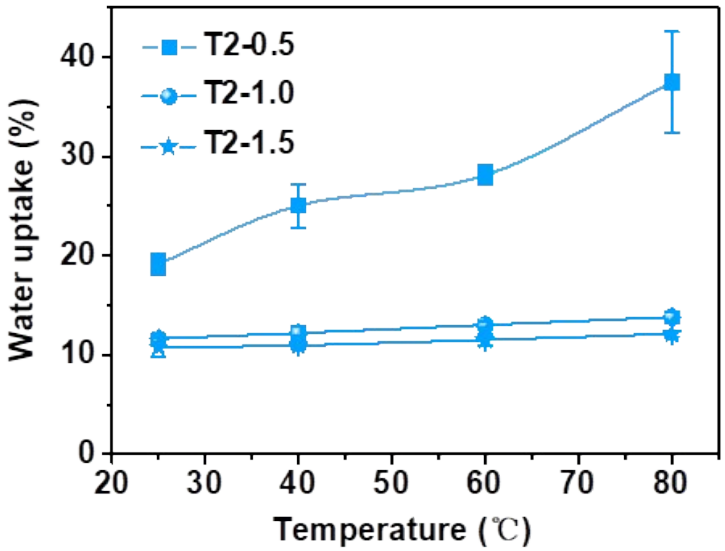

Figure S8. The water uptake of afforded T2 AEMs with different Sp ratios at different temperatures.

Table S1. The polymerization state of T1, T2, and T3 AEMs and their molecular weights.

AEMs	Feed ratio of spatial centers to aromatic hydrocarbon monomers (mol%)	Gelation	M_w (kDa)
PTP	0	No	48.6
T1-0.5	0.5 (Trp)	No	76.4
T1-1.0	1.0 (Trp)	No	86.3
T1-2.0	2.0 (Trp)	No	86.6
T1-3.0	3.0 (Trp)	Partially	-
T2-1.0	1.0 (Sp)	No	87.5
T3-1.0-1.0	1.0 (Trp), 1.0 (Sp)	No	92.7

Note: The polymerization conditions were optimized by changing the feed ratio of Trp or/and Sp. When the feed ratio of Trp was increased to 3 mol%, the gelation occurred during polymerization. When the feed ratio of Sp was increased to 2 mol%, the gelation occurred during polymerization. The molecular weight of the polymers was tested by GPC using DMF (50 mM LiBr) as eluent.

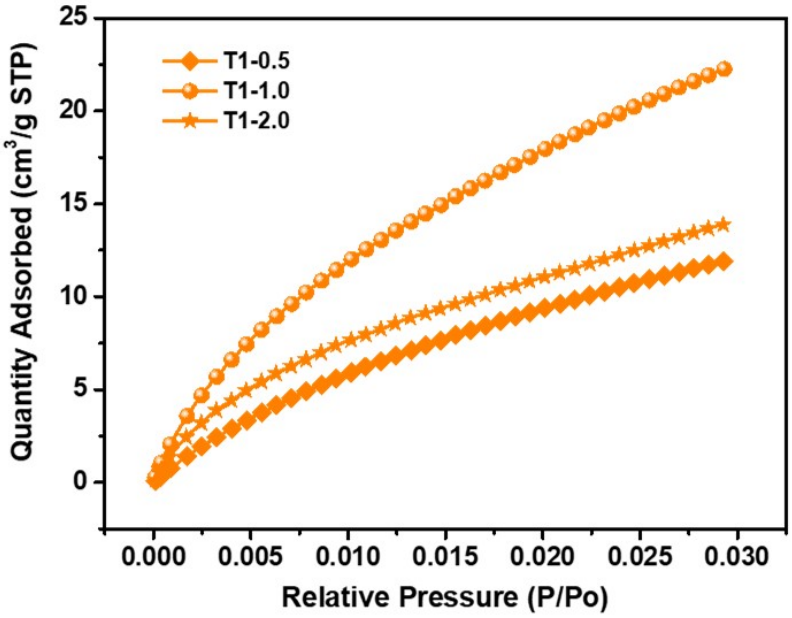

Figure S9. The CO_2 adsorption isotherms of T1-0.5, T1-1.0 and T1-2.0 AEMs at 0 °C.

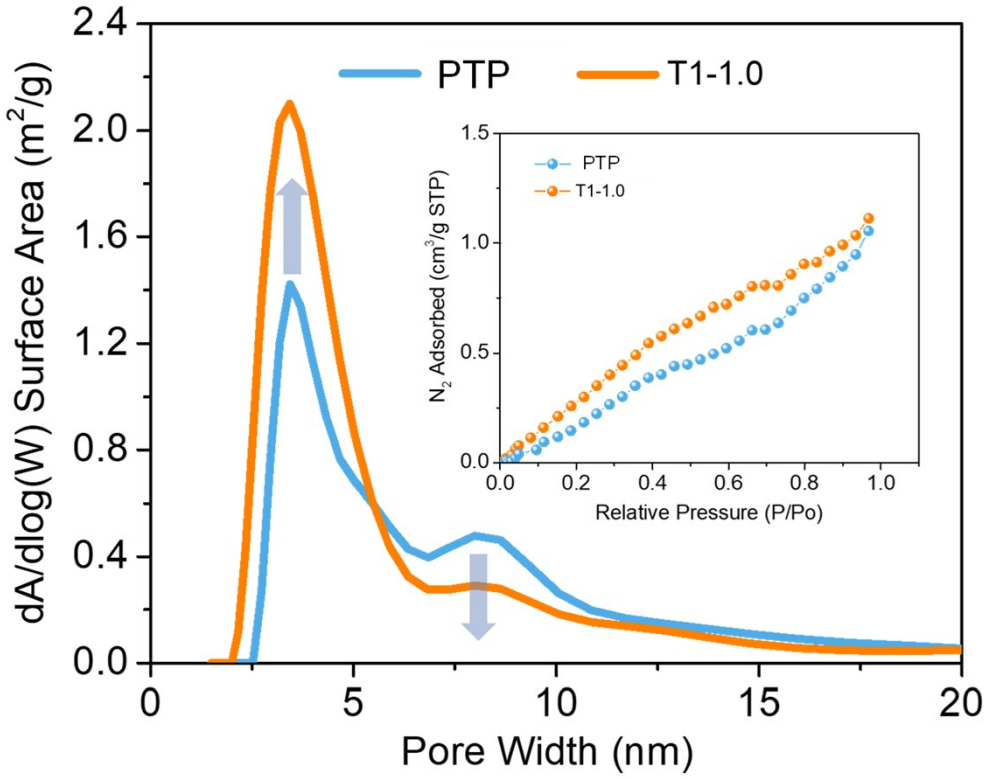

Figure S10. The pore distribution of the T1-1.0 and PTP that is calculated from N_2 adsorption isotherms, inset: its corresponding adsorption isotherms.

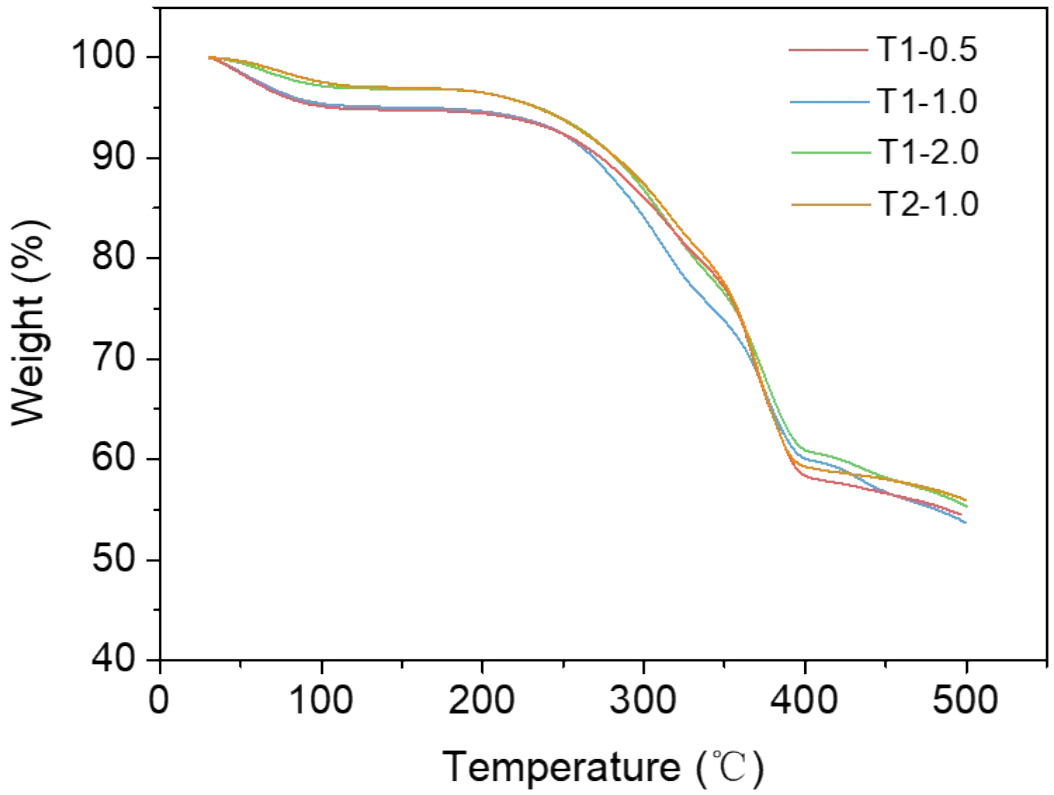

Figure S11. The TGA results of T1-0.5, T1-1.0, T1-2.0, and T2-1.0 AEMs.

Note: Thermogravimetric analysis (TGA) revealed the thermal stability of the PTP and T1 AEMs. In **Figure S11**, the first weight-loss stage between 30 to 150 °C is assigned to dehydration, the second stage between 200 to 350 °C is the decomposition of the amino-functional group, and the further weight loss over 400 °C is the decomposition hydrocarbon backbone.

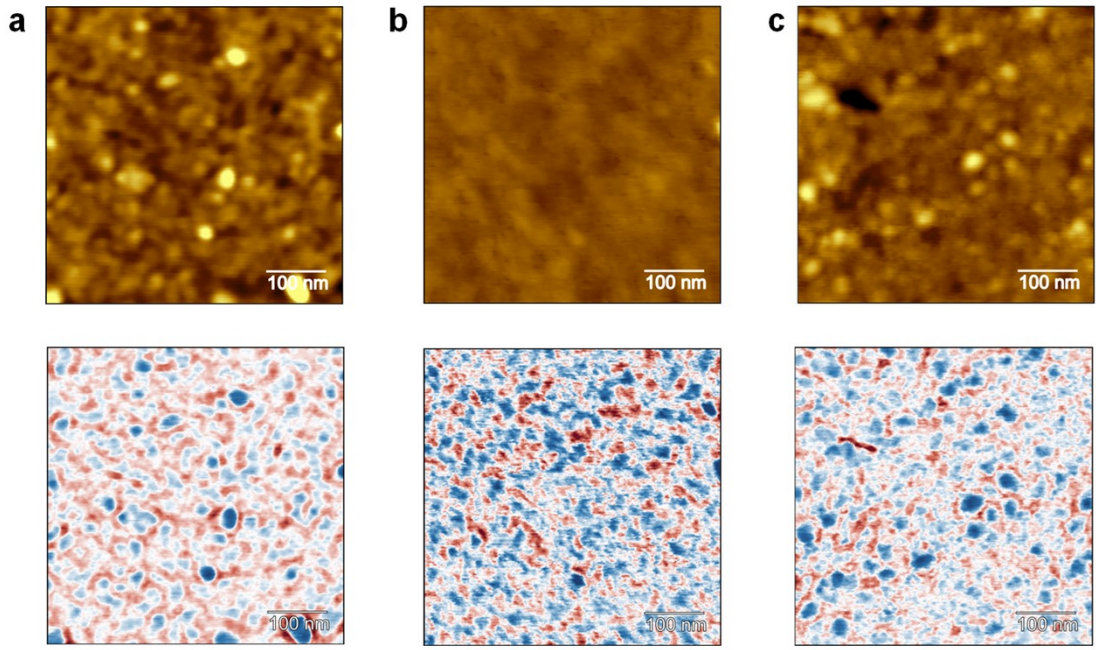

Figure S12. The AFM results of afforded AEMs (***up***, height images; ***down***, phase images): (a) T1-0.5; (b) T1-1.0; (c) T1-2.0.

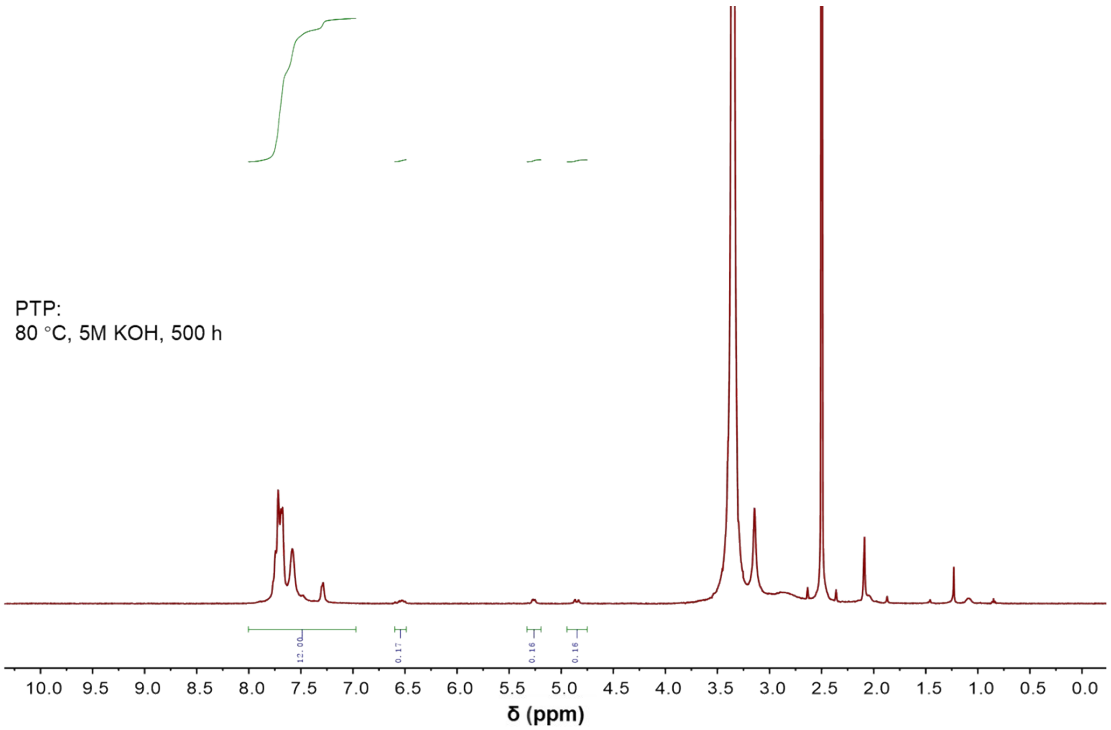

Figure S13. ^{1}H NMR spectrum of PTP membrane after the alkaline stability test in 5 M KOH at 80 °C for 500 h using DMSO-d_6 as the solvent.

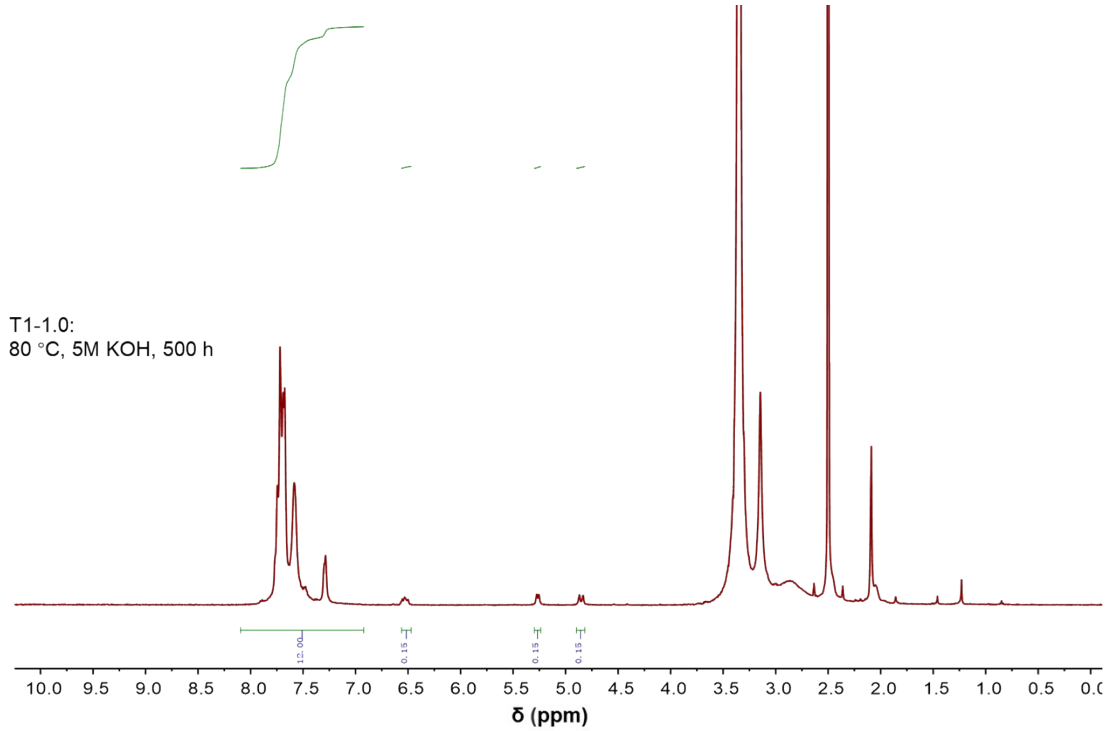

Figure S14. ^{1}H NMR spectrum of T1-1.0 membrane after the alkaline stability test in 5 M KOH at 80 °C for 500 h using DMSO-d_6 as the solvent.

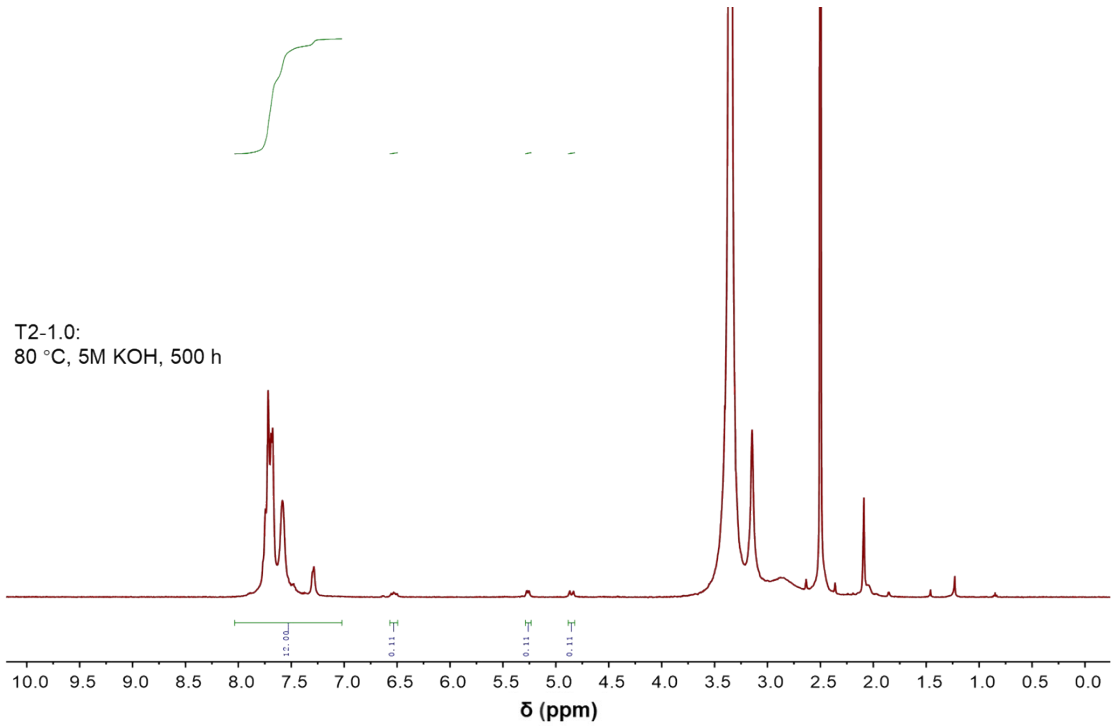

Figure S15. ^{1}H NMR spectrum of T2-1.0 membrane after the alkaline stability test in 5 M KOH at 80 °C for 500 h using DMSO-d_6 as the solvent.

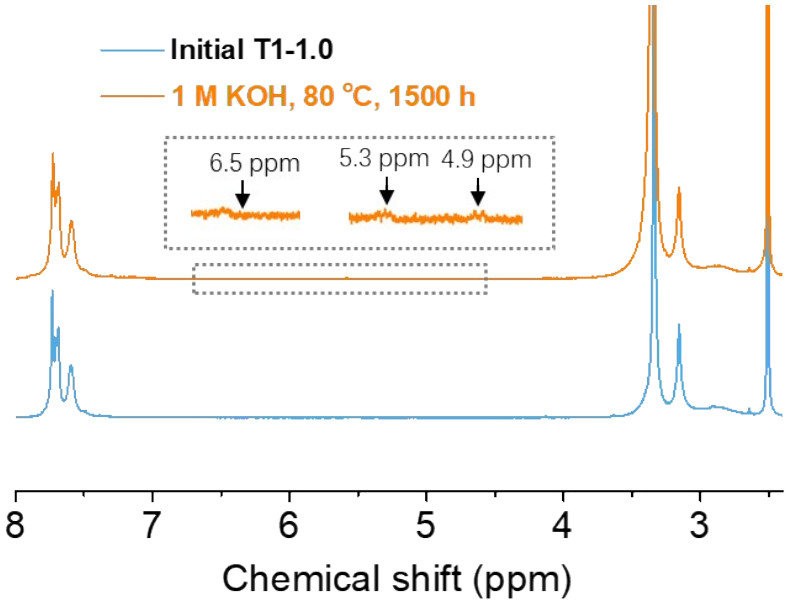

Figure S16. ^{1}H NMR spectra of T1-1.0 membranes before and after the alkaline stability test in 1 M KOH at 80 °C for 1500 h using DMSO-d_6 as the solvent.

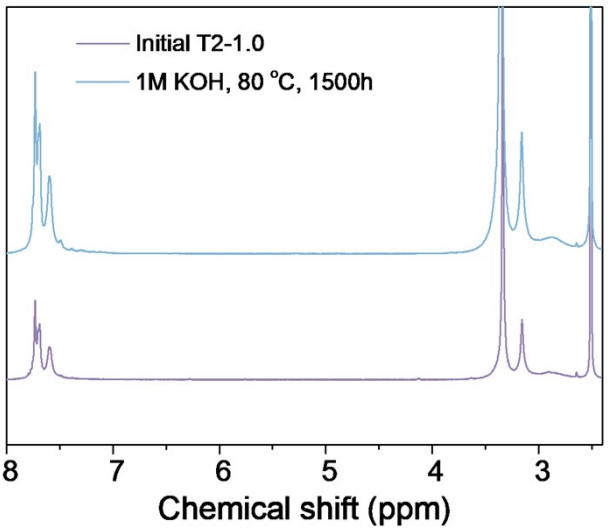

Figure S17. ^{1}H NMR spectra of T2-1.0 membranes before and after the alkaline stability test in 1 M KOH at 80 °C for 1500 h using DMSO-d_6 as the solvent.

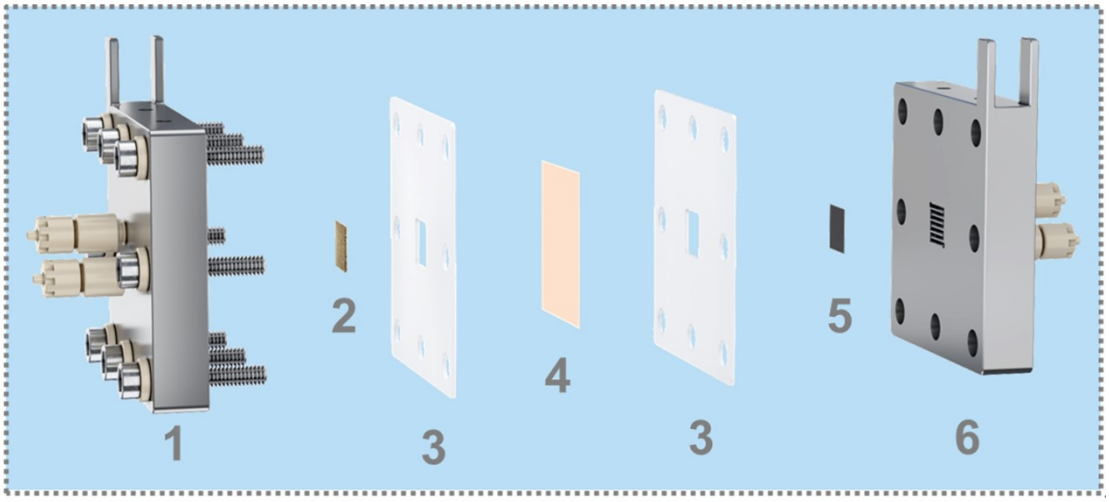

Figure S18. The setup of AEM-WE device. AEM electrolyzer consisting of **1** Plate with flow field (1cm×1cm); **2** anode catalyst; **3** silica gel gasket; **4** AEM; **5** cathode catalyst; **6** backing plate.

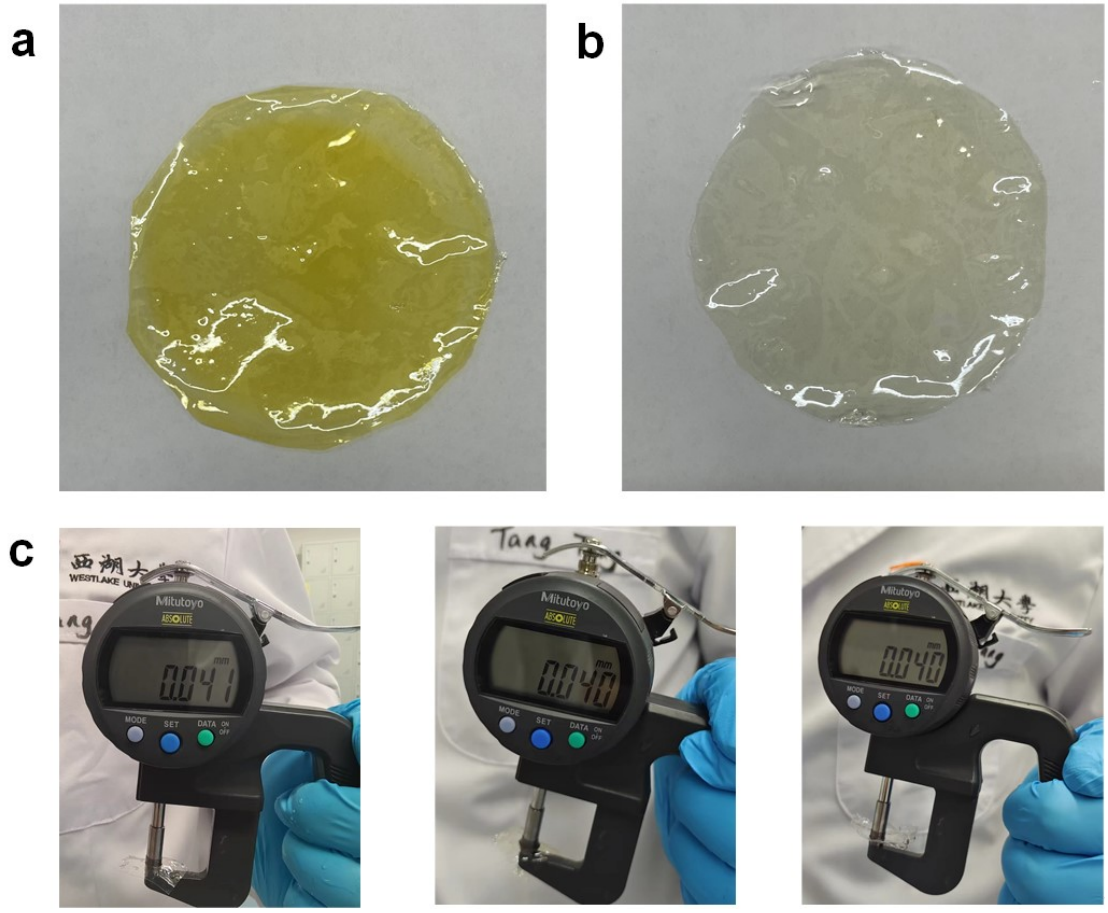

Figure S19. (a) The membrane of T1-1.0 in Cl^- state. (b) The membrane of T1-1.0 in OH^- state. (c) The thickness of T1-1.0 in OH^- state (*left*); the thickness of PTP in OH^- state (*middle*); The thickness of PAP-TP in OH^- state (*right*).

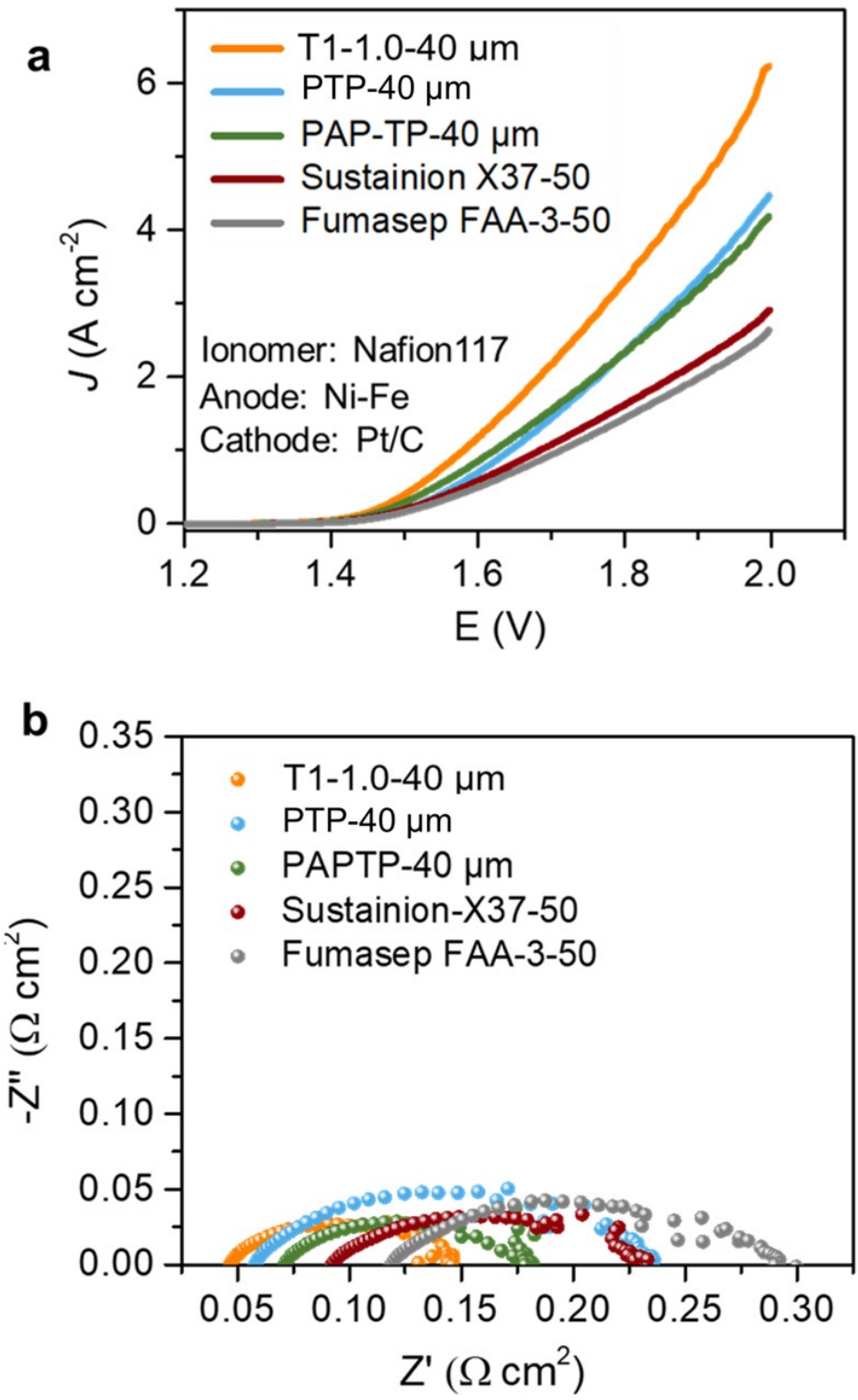

Figure S20. (a) J–V curves and **(b)** EIS spectra of single-cell AEM-WEs using T1-1.0 and different commercially available AEMs at 80 °C. Testing conditions: 1 M KOH, Ni-Fe@NF anode, and 1.0 mg cm^{-2} Pt/C cathode with Nafion as ionomer.

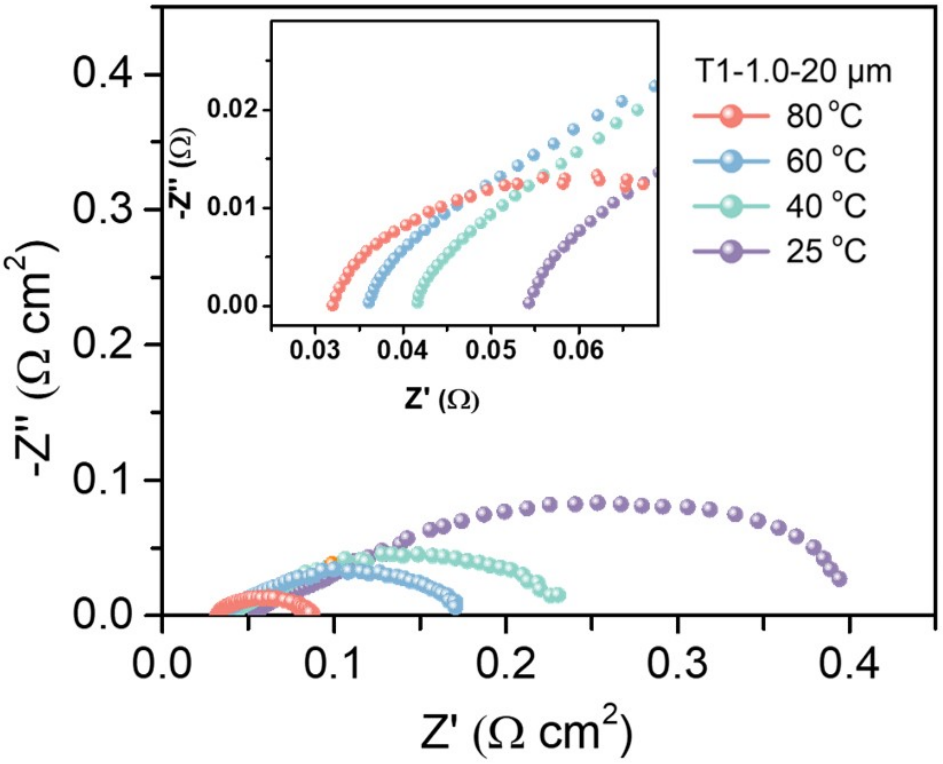

Figure S21. EIS spectra of single-cell AEM-WEs using T1-1.0 (20 μm) as AEMs at 25 °C, 40 °C, 60 °C, and 80 °C. Testing conditions: 1 M KOH feed electrolyte; Ni-Fe anode and Ni-Mo cathode.

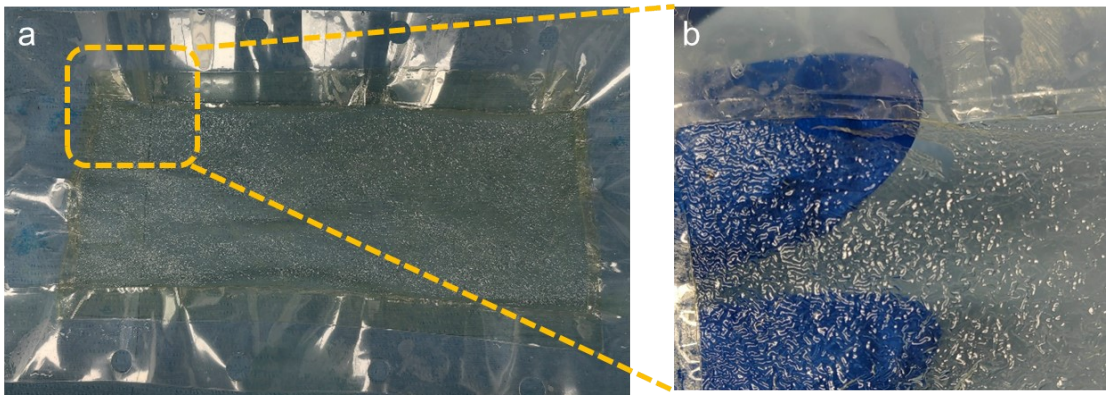

Figure S22. Pictures of the posted T1-1.0 (80 μm) after testing in Lize electrolysis cell.

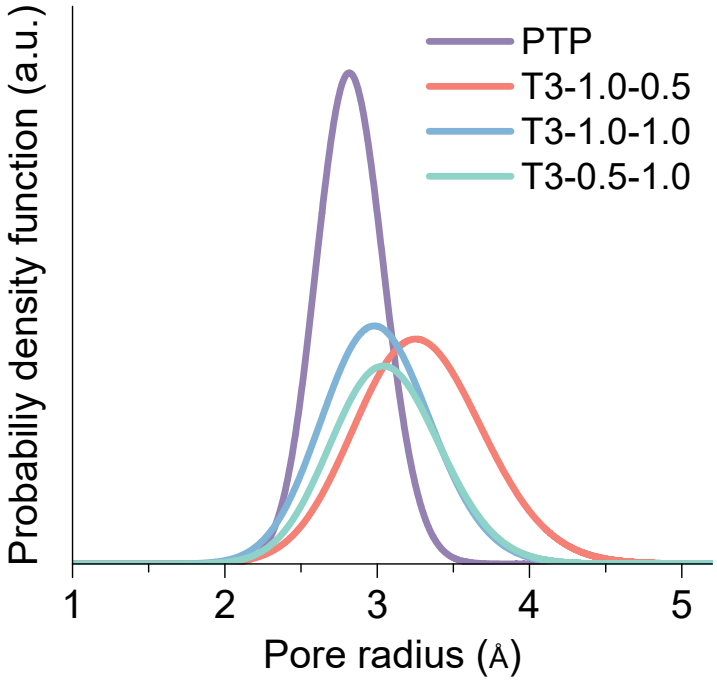

Figure S23. Pore size distribution of PTP, T3-1.0-0.5, T3-1.0-1.0, and T3-0.5-1.0 AEMs obtained from positron annihilation lifetime spectroscopy (PALS).

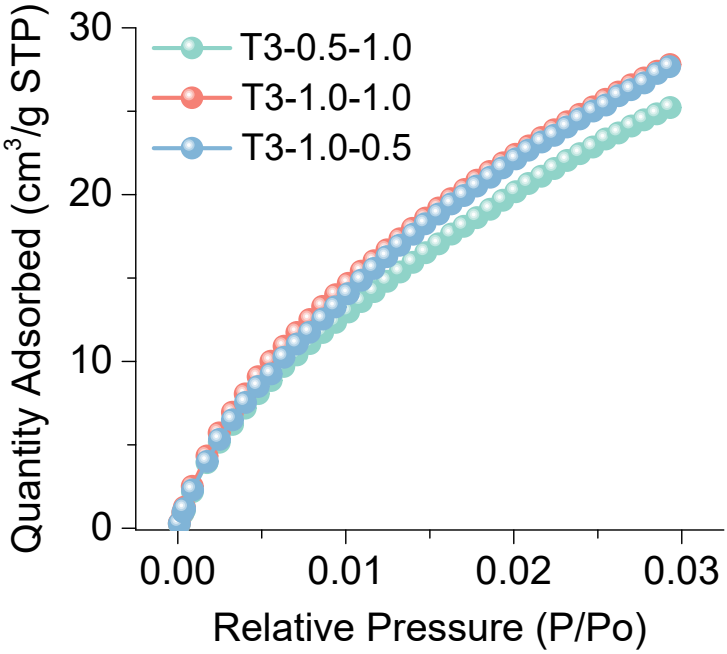

Figure S24. The CO_2 adsorption isotherms of PTP, T3-1.0-0.5, T3-1.0-1.0 and T3-0.5-1.0 AEMs at 0 °C.

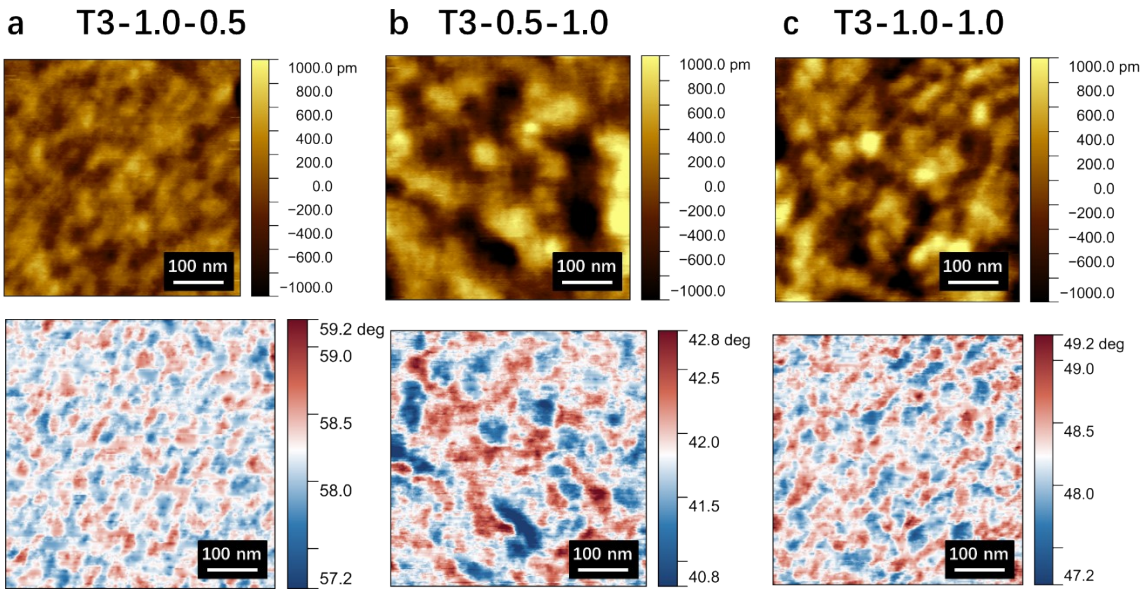

Figure S25. AFM height (***up***) and phase (***down***) images of AEMs **(a)** T3-1.0-0.5; **(b)** T3-0.5-1.0; **(c)** T3-1.0-1.0.

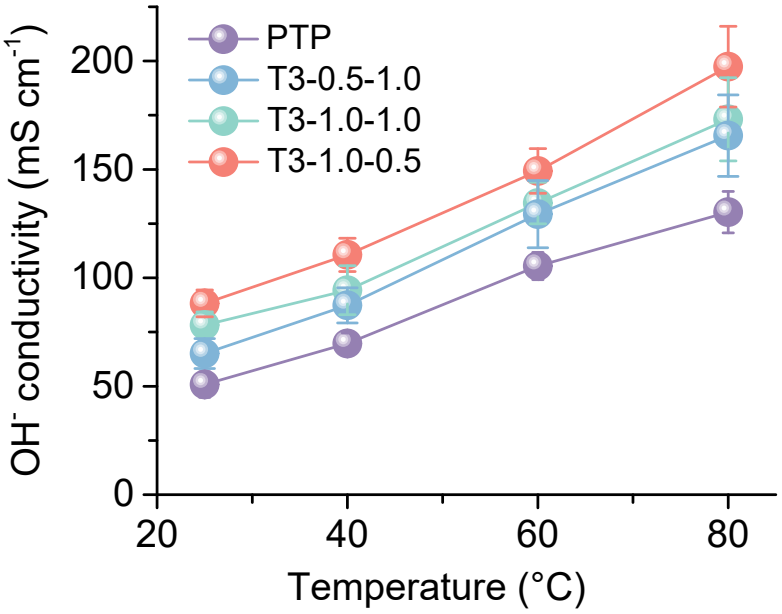

Figure S26. The OH- conductivity of afforded T3 AEMs at different temperatures.

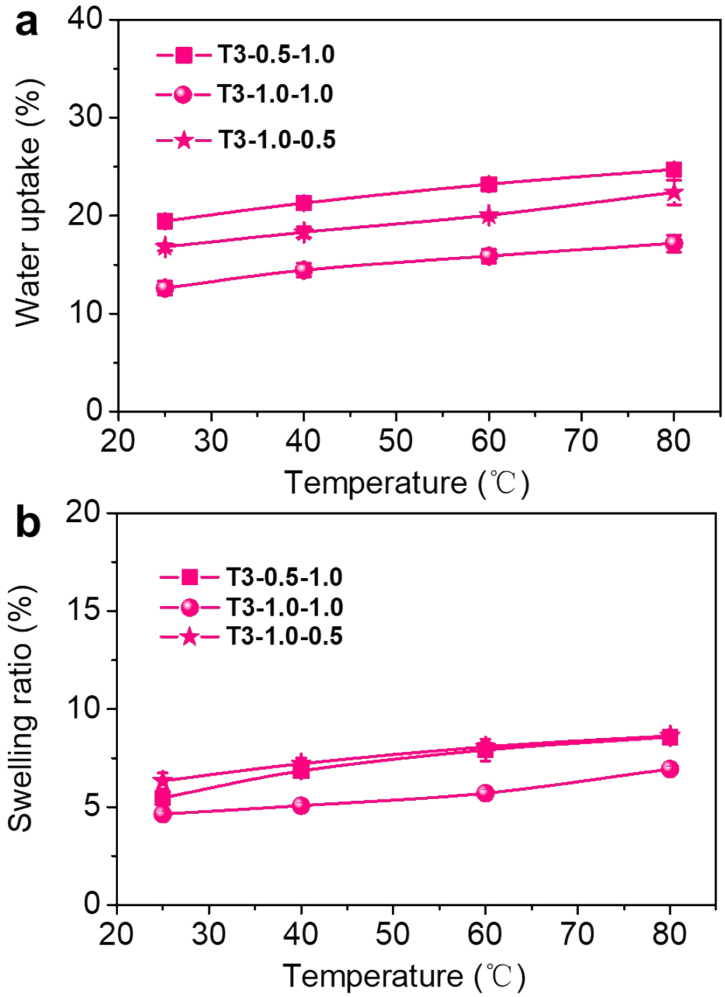

Figure S27. (a) The water uptake of afforded T3 AEMs at different temperatures. (b) The swelling ratio of afforded T3 AEMs at different temperatures.

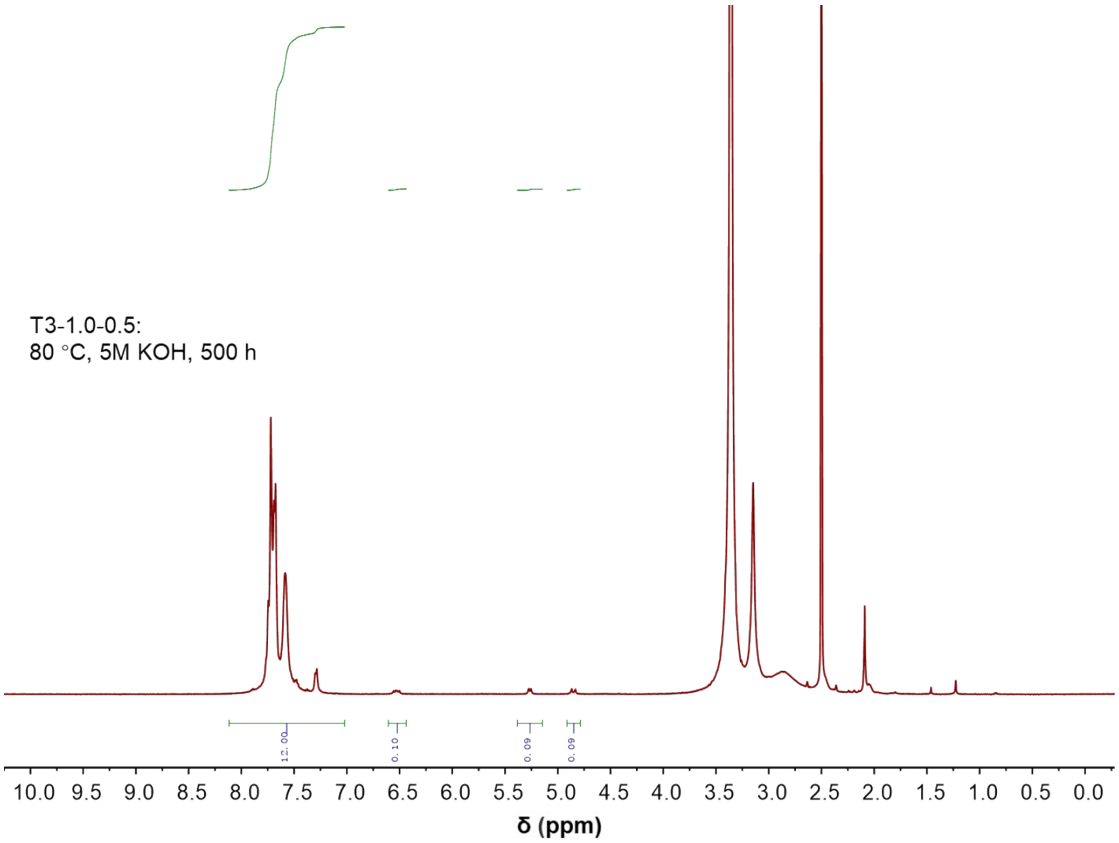

Figure S28. ^{1}H NMR spectrum of T3-1.0-0.5 membrane after the alkaline stability test in 5 M KOH at 80 °C for 500 h using DMSO-d_6 as the solvent.

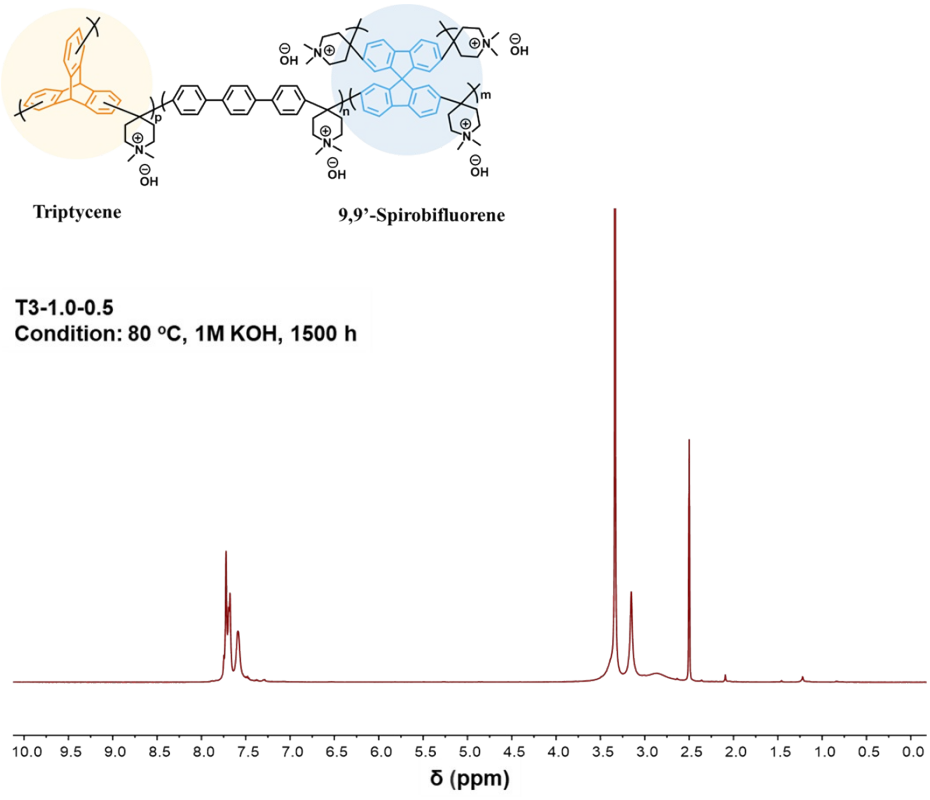

Figure S29. ^{1}H NMR spectrum of T3-1.0-0.5 membrane after the alkaline stability test in 1 M KOH at 80 °C for 1500 h using DMSO-d_6 as the solvent.

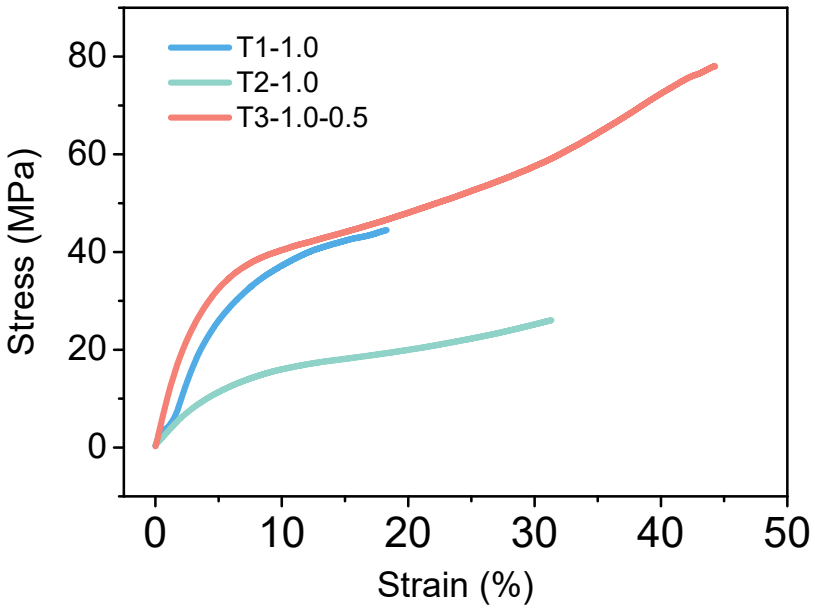

Figure S30. Tensile strength of T1-1.0, T2-1.0 and T3-1.0-0.5 AEMs (in OH^- state) in saturated state after water absorption.

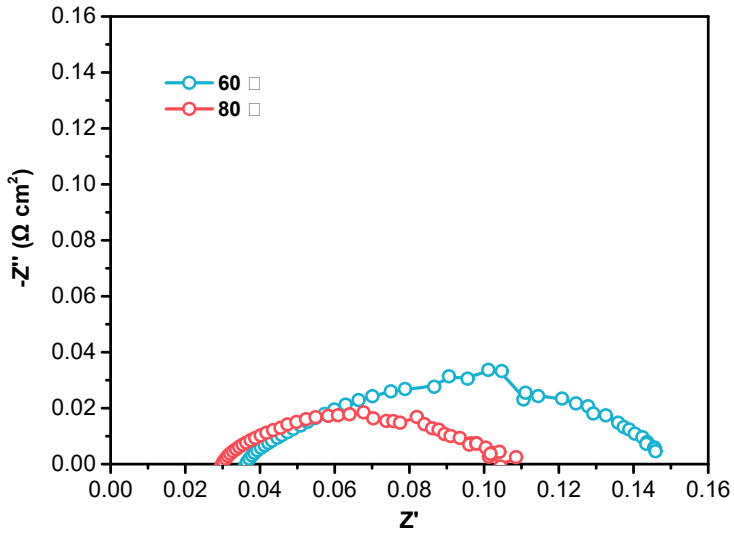

Figure S31. EIS spectra of single-cell AEM-WE using T3-1.0-0.5 (20 μm) as AEM at 60 °C and 80 °C. Testing conditions: 1 M KOH feed electrolyte; Ni-Fe anode and Ni-Mo cathode.

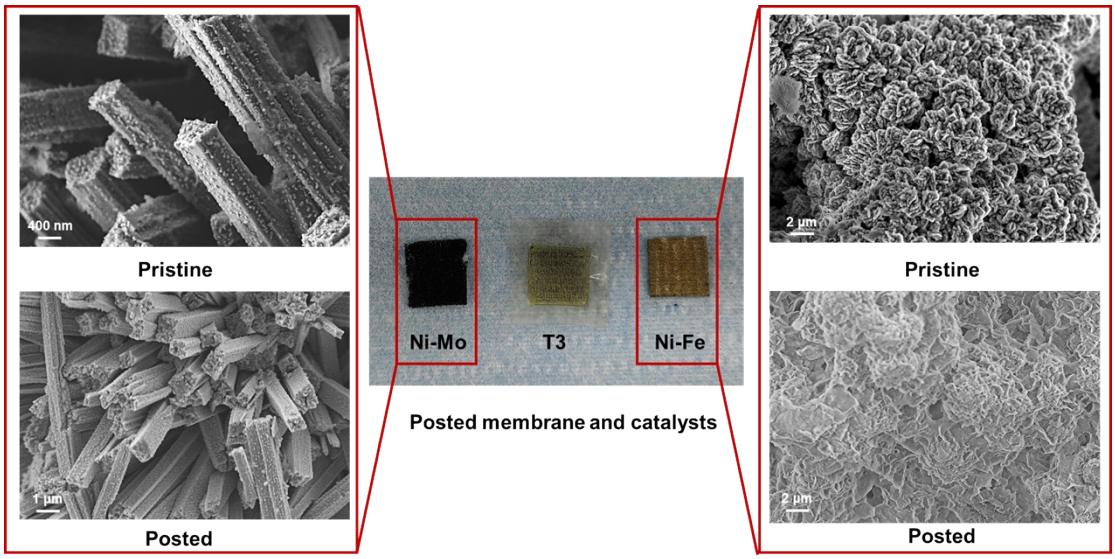

Figure S32. Picture and the SEM figures of the T3-1.0-0.5 membrane, Ni-Fe catalyst and Ni-Mo catalyst after the AEM-WE cell testing for 530 h. AEM-WE testing conditions: 60 °C; 1 M KOH feed electrolyte; Ni-Fe anode and Ni-Mo cathode.

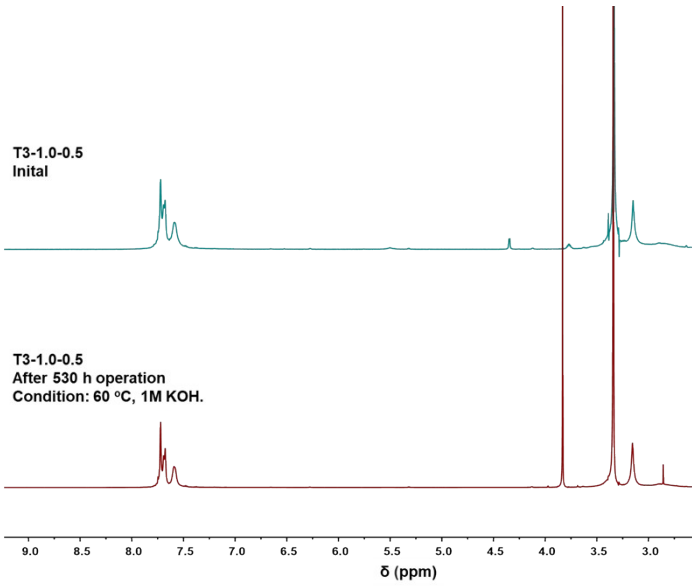

Figure S33. ^{1}H NMR spectra of T3-1.0-0.5 membrane before and after the AEM-WE cell testing using DMSO-d_6 as the solvent. AEM-WE testing conditions: 60 °C; 1 M KOH feed electrolyte; Ni-Fe anode and Ni-Mo cathode.

Note: The anion exchange membrane in contact with the flow field region is removed and immerged in a 1M KI solution, and then rinsed several times with deionized water. After drying, thus treated membrane is dissolved in a DMSO solution and to produce a new film. This new film is redissolved in a deuterated reagent DMSO-d6 for ^{1}H NMR analysis.

Figure S34. Picture of the T3-1.0-0.5 membranes after the industrial-scale AEM-WE cell testing for 210 h. AEM-WE testing conditions: 60 °C; 1 M KOH feed electrolyte; Ni-Fe anode and Ni-Mo cathode.

Table S2. The summary and comparison of representative AEM-WEs performance and stability.

Cathode	Anode	Membrane	T/ °C	*J*/A cm^{-2}	E/V	Stability test	Ref.
Ni-Mo	Ni-Fe	T1-1.0	80	8.0	2.00	1200 h @ 1 A cm^{-2}	**This work**
Ni-Mo	Ni-Fe	T3-1.0-0.5	80	8.4	2.00	520 h @ 2 A cm^{-2}, 60 °C	
Pt/C	IrO_2	PFTP-13	80	7.68	2.00	1100 h @ 0.5 A cm^{-2}	[S13]
Ni-Fe	Ni-Fe	PFTP-13	60	1.00	1.94	1000 h @ 0.5 A cm^{-2}	
Pt/C	Ni_2P/Ni_7S_6	FAA-3PE-30	75	1.00	1.88	140 h @ 1.0 A cm^{-2}	[S14]
PtRu/C	NiFe	HTMA-DAPP	85	5.30	1.80	—	[S15]
NiMo-NH_3/H_2	Fe-NiMo-NH_3/H_2	Sustainion X37–50	80	1.00	1.57	25 h @ 0.5 A cm^{-2}	[S16]
VCoP-2	VCoP-2	PBI	80	4.20	2.00	600 h @ 1.00 A cm^{-2}	[S17]
3-Co_3S_4 NS/NF	$Cu_{0.81}Co_{2.19}O_4$	Sustainion X37-50	45	0.431	2.00	10 h @ 0.5, 4.2 mV h^{-1}↑	[S18]
NiFeCo	$NiFe_2O_4$	Sustainion X37-50	60	1.00	2.01$^{\alpha}$	—	[S19]
Raney Ni	$NiFe_2O_4$	Sustainion Grade T	60	1.00	1.85	12180 h @ 1.00 A cm^{-2}	[S20]
Ni-MoO_2	$Ni_{0.6}Co_{0.2}Fe_{0.2}$	FAA-3-PE-30	50	1.15	2.00	65 h @ 0.50 A cm^{-2} in 0.1 M KOH	[S21]
NiCoO-NiCo/C	$Cu_{0.75}Co_{2.25}O_4$	Sustainion X37–50	50	0.50	1.85	10 h @ 0.44 A cm^{-2}	[S22]

		Grade T					
$MoNi_4/MoO_2$	Ni_2P@FeP O_xH_y	Sustainion X37–50	60	1.00	1.84	72 h @ 0.48 A cm^{-2}	[S23]
NiFeCo	$NiFe_2O_4$	C-IL-100	80	0.88	2.20	8 h @ 0.10 A cm^{-2}	[S24]
Pt/C/CP	$Co(OH)_x$/Ag/$Co(OH)_2$	Sustainion X37-50	50	0.60	1.80	24 h @ 0.60 A cm^{-2}	[S25]
60% Pt/C	Ir black	AF1-HNN8-50	60	1.00 2.00	1.70 1.82	17 h @ 0.50 A cm^{-2}	[S26]

[S1] J. Zhang, T. Wang, P. Liu, Z. Liao, S. Liu, X. Zhuang, M. Chen, E. Zschech, X. Feng, *Nat. Commun.* **2017**, 8, 15437.

[S2] W. Zhao, H. Xu, H. Luan, N. Chen, P. Gong, K. Yao, Y. Shen, Y. Shao, *Adv. Energy Mater.* **2022**, 12, 2102372.

[S3] (2012) Discovery Studio Visualizer Software, Version 4.0. http://www.accelrys.com.

[S4] J. C. B. Phillips, R. Wang, W. Gumbart, J., E. V. Tajkhorshid, E. Chipot, C. Skeel, R. D. Kalé, L. Schulten, K. *J. Comput. Chem.* **2005**, 26, 1781-1802.

[S5] K. H.r Vanommeslaeghe, E. Acharya, C. Kundu, S. Zhong, S. Shim, J. E. Darian, E. Guvench, O. Lopes, P. Vorobyov, I. MacKerell, *J Comput Chem*, **2010**, 31, 671-690.

[S6] T. Darden, D. York, L. *J.* Pedersen, *Chem. Phys.* **1993**, 98, 10089-10092.

[S7] W. G. Hoover, A. J. C. Ladd, B. Moran, *Phys. Rev. Lett.* **1982**, 48, 1818.

[S8] J. P. Ryckaert, G. Ciccotti, H. J. C. Berendsen, *J. Comp. Phys.* **1977**, 23, 327.

[S9] S. E. Feller, Y. Zhang, R. W. Pastor, B. R. Brooks, *J. Chem. Phys.* **1995**, 103, 4613−4621.

[S10] W. Humphrey, A. Dalke, K. Schulten, *J. Mol. Graph.* **1996**, 14, 33-38.

[S11] L. Sarkisov, R. Bueno-Perez, M. Sutharson and D. Fairen-Jimenez, *Chem. Mater.* **2020**, 32, 9849–9867.

[S12] T. Giorgino, *J. open source softw.* **1698**, 4, 41.

[S13] N. Chen, S. Y. Paek, J. Y. Lee, J. H. Park, S. Y. Lee, Y. M. Lee, *Energy Environ. Sci.* **2021,** 14, 6338–6348.

[S14] F.-L. Wang, N. Xu, C.-J. Yu, J.-Y. Xie, B. Dong, X.-Y. Zhang, Y.-W. Dong, Y.-L. Zhou, Y.-M. Chai, *Appl. Catal. B-Environ.* **2023***,* 330, 122633.

[S15] D. Li, Y. Lin, A. Serov, H. T. Chung, E. J. Park, W. Zhu, B. Zulevi, Y. S. Kim, *Nat. Energy* **2020**, 5, 378–385.

[S16] P. Chen, X. Hu, *Adv. Energy Mater.* **2020,** *10*, 2002285.

[S17] L. Wan, Z. Xu, Q. Xu, P. Wang, B. Wang, *Energy Environ. Sci.* **2022**,15, 1882–1892.

[S18] Y. S. Park, J. H. Lee, M. J. Jang, J. Jeong, S. M. Park, W.-S. Choi, Y. Kim, J. Yang, S. M. Choi, *Int. J. Hydrogen Energy* **2020**, 45, 36–45.

[S19] I. V. Pushkareva, A. S. Pushkarev, S. A. Grigoriev, P. Modisha, D. G. Bessarabov, *Int. J. Hydrogen Energy* **2020,** 45, 26070–26079.

[S20] B. Motealleh, Z. Liu, R. I. Masel, J. P. Sculley, Z. Richard Ni, L. Meroueh, *Int. J. Hydrogen*

Energy **2021,** *46*, 3379.

[S21] A. Y. Faid, A. O. Barnett, F. Seland, S. Sunde, *ACS Applied Energy Materials* **2021,** 4, 3327–3340.

[S22] Y. S. Park, J. Jeong, Y. Noh, M. J. Jang, J. Lee, K. H. Lee, D. C. Lim, M. H. Seo, W. B. Kim, J. Yang, S. M. Choi, *Applied Catalysis B-Environ.* **2021,** 292, 120170.

[S23] A. Meena, P. Thangavel, D. S. Jeong, A. N. Singh, A. Jana, H. Im, D. A. Nguyen, K. S. Kim, *Appl. Catal. B-Environ.* **2022,** *306*, 121127.

[S24] X. Wang, R. G. H. Lammertink, *J. Mater. Chem. A* **2022,** *10*, 8401.

[S25] W. Guo, J. Kim, H. Kim, G. H. Han, H. W. Jang, S. Y. Kim, S. H. Ahn, *J. Alloy Compd.* **2021**, 889, 161674.

[S26] P. Fortin, T. Khoza, X. Cao, S. Y. Martinsen, A. Oyarce Barnett, S. Holdcroft, *J. Power Sources* **2020**, 451, 227814.